Article

Development and Characterisation of Arabinoxylan-Based Composite Films

Joana Salvada [1], Bhavna Alke [1], Carla Brazinha [1], Vítor D. Alves [2,*] and Isabel M. Coelhoso [1]

1   LAQV-Requimte, Department of Chemistry, NOVA School of Science and Technology, NOVA University of Lisbon, 2829-516 Caparica, Portugal; j.salvada@campus.fct.unl.pt (J.S.); b.alke@campus.fct.unl.pt (B.A.); c.brazinha@fct.unl.pt (C.B.); imrc@fct.unl.pt (I.M.C.)
2   LEAF—Linking Landscape, Environment, Agriculture and Food, Associated Laboratory TERRA, Instituto Superior de Agronomia, Universidade de Lisboa, 1349-017 Lisboa, Portugal
*   Correspondence: vitoralves@isa.ulisboa.pt; Tel.: +351-365-3546

Abstract: In the last decades, the overuse of synthetic polymers in the packaging industry has become a serious global environmental problem due to their nonbiodegradability. To overcome this issue, attention has been driven to study alternative materials, namely the use of biodegradable biopolymers extracted from agro-industrial residues, as materials for food packages. In this work, the polysaccharide arabinoxylan, previously extracted from corn fibre by alkaline hydrolysis, was used to produce composite and multilayer films. The composite films were produced by casting an oil-in-water emulsion with different quantities of oleic acid, while the multilayer films (beeswax-arabinoxylan-beeswax) were manufactured by submerging the arabinoxylan films in a beeswax solution. Both film types, along with a film composed only of arabinoxylan, were characterised in terms of their antioxidant activity, optical and mechanical properties, surface hydrophobicity, and barrier properties against water vapour (WVP), gases, and ultraviolet-visible (UV-vis) radiation. All the films developed were soluble in water. The multilayer films were more advantageous than the emulsion-based ones due to their enhanced barrier properties against water vapour (WVP = 0.58×10^{-11} mol/m·s·Pa), oxygen (with a permeability of 3.28×10^{-12} mol·m^{-1}·s^{-1}·Pa^{-1}) and UV-vis radiation and higher values of water contact angle ($92.43°$), tensile stress (4.11 MPa), and Young's modulus (15.96 MPa). The films developed, especially the multilayer ones, showed a good potential to produce flexible packages for low-water-content food products (e.g., several types of nuts).

Keywords: arabinoxylan; biodegradable films; oleic acid; beeswax; emulsion; food packaging

1. Introduction

Over the past few years, we have witnessed a massive acceleration in the need for food-packaging alternatives, as the problems of using nonbiodegradable polymers have become inevitably more noticeable [1]. Plastic materials have dominated the packaging market for some time now since they are extremely versatile with appealing features such as lightness, good barrier proprieties, low cost, durability, and moldability, among others. In Europe, 40% of the plastic market is used in the food-packaging sector [2], and over 50% of all European goods are packaged in plastic containers [3]. The raw materials used for plastic are most commonly obtained from nonrenewable resources, including fossil fuel industry products, because they can be produced in higher quantities at a relatively low cost [4]. Due to their biological resistance and excellent water barrier properties, the most common polymers used in plastic packaging are polyethylene (PE), polypropylene (PP), polyethylene terephthalate (PET), polyvinyl chloride (PVC), high-density polyethylene (HDPE), low-density polyethylene (LDPE), and polystyrene (PS) [5,6].

Even though plastic packaging has many advantages, as mentioned above, it is extremely wasteful and has been proved to have a negative impact on the earth's ecosystems. In 2015, 407 million tonnes of plastics were produced worldwide, and of those,

302 million tonnes were discarded as waste [4]. Additionally, in 2015, the majority of global plastic waste, about 55%, was sent to landfills or disposed of in the environment, while 25% was incinerated, and only 20% was recycled [7].

Bearing all of this in mind and considering that plastic is made from nonrenewable resources and is nonbiodegradable, it may withstand the test of time, posing a threat not only to human health but also to the environment [6]. Therefore, it is crucial that new forms of food packaging are created to replace the unsustainable designs upon which modern life depends. A possible solution lies in the use of biodegradable, preferably edible, food-packaging films and coatings based on biopolymers obtained from agricultural commodities or food-waste products, such as seeds, peels and skins, husks, unripe or damaged fruits, vegetables, or cereals [8].

The most-used materials in the production of bio-based films and thin membranes are biopolymers extracted from biomass, such as proteins (e.g., whey protein, gluten, gelatin, zein, and legume seed proteins) [9] and polysaccharides (e.g., chitosan, alginate, pectin, glucomannans, cellulose, starch, pullulan, and carrageenan) [10–13], as well as compostable polymers such as polycaprolactone and polylactic acid [14–16].

Upon the production of polysaccharide-based films, a wide range of hydrophobic compounds has been added to films' formulations in order to increase their barrier properties to water. These compounds include animal and vegetable oils and fats, waxes, natural resins, and essential oils, for example [17–19]. Hydrophobic compounds can be added to polysaccharide-based film through two types of film preparation: either by forming a bilayer or multilayer film in which the oil acts as a laminate over one or both films' surfaces, or by dispersing homogeneously and entrapping the oil in the polysaccharide's matrix in the form of an emulsion [17–19]. In general, bilayer and multilayer films are more effective barriers against water vapour transfer than emulsion-based films. On the other hand, the preparation of bilayer or multilayer films is more time-consuming, as there are several steps (two casting and two drying steps), and the lipid coatings tend to tear off during storage, which results in a nonuniform surface with pinholes or cracks [17].

Among the polysaccharides that have been tested are arabinoxylans (AXs). They are extracted from a wide range of cereal crops, such as wheat, rye, barley, oat, rice, sorghum, and corn. Agricultural side streams can contain arabinoxylans that make up 40% of their dry weight [20]. AXs consist of a linear chain of β-(1-4)-linked-D-xylopyranosyl units with α-L-arabinofuranosyl residues as side chains attached to the main xylose backbone at the O-2, O-3, or O-2,3 positions, resulting in four different structures (monosubstituted at O-3 or O-2, disubstituted at O-2,3, and unsubstituted). Ferulic acid is commonly esterified on the O-5 position of arabinose branches [20]. Several studies have demonstrated their biological properties, such as antioxidant capacity, prebiotic properties, and more recently, anticancer properties. In fact, phenolic acids bound to arabinoxylan, such as ferulic acid (FA), exhibit antioxidant activity, which has beneficial effects against chronic and cardiovascular diseases, cancer, diabetes, inflammatory diseases, and ageing [21]. In what concerns AX application in bio-based films, some works have been reported using the biopolymer with or without chemical modifications [22,23]. In addition, works regarding composite AX-oils/fatty acids films have been also carried out [24,25]. However, there is still a lack of knowledge concerning the development of composite AX films, either emulsion-based (combining with oils or fatty acids) or multilayer (combining with solid waxes at ambient temperature).

In a first work, an arabinoxylan fraction extracted from corn fibre using alkaline hydrolysis was purified [23] and used to develop biodegradable films [26]. The aim of the present study is to go further on the development of emulsion-based (with oleic acid) and multilayer (with beeswax) films. The films were characterised in terms of their optical and mechanical (Young's modulus, tensile stress, and elongation at break) properties, surface hydrophobicity, antioxidant activity, barrier properties (against water vapour, gases, and ultraviolet-visible radiation), and surface and cross-section morphologies, envisaging their application in packages for low-water-content food products (e.g., walnuts or peanuts).

2. Materials and Methods

2.1. Materials

To carry out this work, corn fibre was obtained from the company Copam (Companhia Portuguesa De Amidos, S.A., Lisbon, Portugal) and was used to extract the arabinoxylan. For the films' formulation, various reagents were used: the plasticiser glycerol (>99%, Sigma-Aldrich, St. Louis, MI, USA), the non-ionic polysorbate surfactant Tween® 20 (Sigma-Aldrich, St. Louis, MI, USA), extra-pure oleic acid (>99%, Merck, Darmstadt, Germany), beeswax (obtained from the apiary at the Instituto Superior de Agronomia, Portugal), and ethanol (>99.8%, Riedel-de-Haën, Honeywell, Seelze, Germany). For the water vapour permeability, sodium chloride (99.5%, José Manuel Gomes dos Santos LDA, Odivelas, Portugal) and magnesium chloride (LabChem, Laborspirit, Loures, Portugal) were used. To determine the antioxidant activity, acetate buffer (99.5%, Riedel-de-Haën, Seelze, Germany), TPTZ (2.4.6-Tri(2-pyridyl)-1.3.5-triazine) (98%, Alfa Aesar, Thermo Fischer Scientific, Lancashire, United Kingdom), hydrogen chloride (>37%, Honeywell, Wien, Austria), and ferric chloride (98%, PanReac, Barcelona, Spain) were used. Oxygen (99.999%, Praxair Portugal Gases SA, Maia, Portugal) and carbon dioxide (99.998%, Praxair Portugal Gases S.A., Maia, Portugal) were also used.

2.2. Extraction of Arabinoxylan

Arabinoxylan was extracted from the corn fibre with mild alkaline hydrolysis using a solution of 0.25 M NaOH for 7 h at 30 °C under stirring, followed by centrifugation. The resulting extract was purified with an ultrafiltration membrane hollow-fibre unit (UFP-100-C-5A, from GE Healthcare, Chicago, IL, USA) in a continuous diafiltration process under controlled temperature and permeate flux conditions [23]. Finally, the purified extract was collected and stored at 4 °C, after which it was frozen and later freeze-dried. The purified lyophilised extract, with a fibrous appearance, was preserved in vacuum-sealed plastic bags and kept at −20 °C until used.

2.3. Characterisation of the Emulsion Phases in Terms of Interfacial Tension

To determine which would be the most suitable concentration of Tween 20 in water to produce a good emulsion, different aqueous solutions with increasing concentrations of Tween 20 were prepared to measure the interfacial tension between these aqueous solutions and oleic acid. All the solutions with Tween 20 were left under stirring overnight to allow complete dissolution. The interfacial tension was measured three times for each solution at room temperature in accordance with the pendant drop method using a Drop Shape Analyser—DSA25 (Krüss, Hamburg, Germany) and Advance software to analyse the results.

2.4. Preparation of the Arabinoxylan Films

The arabinoxylan films were prepared using the casting method and following the procedure from Weng et al. [26] with slight alterations. The purified lyophilised extract was dissolved in distilled water (2% (*w/v*)) under stirring at 45 °C until complete dissolution. Then, glycerol (30% (*w/w*, AX basis)) was added, and the solution was left under stirring at the same temperature for a further 10 min. Volumes of 10 or 40 mL were cast in 50 or 100 mm diameter Teflon dishes, respectively. These were then placed overnight in a 35 °C oven (Binder, Tuttlingen, Germany) or until completely dried and ready to peel. Once peeled, they were placed and sealed in glass petri dishes and stored at room temperature (around 20 °C) in the dark.

2.5. Preparation of the Emulsified Arabinoxylan Films

After the dissolution of glycerol, the solution was cooled to room temperature, and Tween 20 (1% (*w/w*)) was added. The mixture was left under stirring overnight to allow complete dissolution. Next, different amounts of oleic acid (0.25, 0.5, 0.75, and 1% (*w/w*)) were added, and the mixtures were homogenised for 10 min at 10,000 rpm using an Ultra-

Turrax homogeniser (T25 basic Ultra-Turrax, IKA Labortechnik, Janke & Kunkel, Staufen, Germany). The obtained emulsions were set aside until all the air bubbles and foam that resulted from the previous step vanished. Volumes of 10 mL or 40 mL were cast in 50 mm or 100 mm diameter Teflon dishes, respectively. These were then placed overnight in a 35 °C oven (Binder, Tuttlingen, Germany) or until dried and ready to peel. After peeling, they were placed and sealed in glass petri dishes and stored at room temperature (around 20 °C) in the dark.

2.6. Preparation of the Multilayer Arabinoxylan Films

A solution of beeswax was prepared following the procedure from Velickova et al. [17] with minor modifications. First, beeswax (2% (*w/v*)) was mixed with Tween 20 (25% (*w/w*$_{beeswax}$)) in ethanol under stirring at 70 °C until all the beeswax was dissolved. Then, arabinoxylan films prepared as described in Section 2.5 with the intended size and shape were coated on both sides by dipping in the heated wax solution for 10 s. Lastly, they were left at room temperature overnight to dry and were then placed and sealed in glass petri dishes and stored at room temperature (around 20 °C) in the dark.

2.7. Characterisation of the Films

Characterisation was performed for the control film (sample 1, Table 1) and the emulsion-based films (samples 2 to 5, Table 1), as well as for the arabinoxylan films coated with beeswax (sample 6, Table 1).

Table 1. Composition of each sample for the film characterisation.

Sample	AX (*w/v*)	Glycerol (*w/w*, AX basis)	Tween 20 (*w/w*)	Oleic Acid (*w/w*)	Beeswax Coating
1	2%	30%	-	-	-
2	2%	30%	1%	0.25%	-
3	2%	30%	1%	0.5%	-
4	2%	30%	1%	0.75%	-
5	2%	30%	1%	1%	-
6	2%	30%	-	-	x

2.7.1. Thickness Measurement

The thickness of the films was measured with a digital micrometer (Digimatic Micrometer, Mitutoyo, Kawasaki, Japan) in five different places for each film.

2.7.2. Colour Measurement

The colour of each film was measured using a colourimeter (Chroma Meter CR-300, Minolta, Tokyo, Japan) with the CIE L^* a^* b^* colour system. This system represents the quantitative relationships of colours on three axes: L^* stands for lightness, ranging from 0 (black) to 100 (white); a^* represents the red-green coordinate, varying from positive (red) to negative (green); and b^* is the yellow-blue coordinate, also varying from positive (yellow) to negative (blue).

The hue ($h°$) refers to the absorbance or reflection of specific wavelengths of light and is defined by the angle on the chromaticity axes (axes a^* and b^*). This parameter can be calculated using Equations (1), (2), or (3):

$$h^o = \arctan\left(\frac{b^*}{a^*}\right) \times \frac{180}{\pi}, \text{ for } a^* > 0 \text{ and } b^* > 0 \tag{1}$$

$$h^o = \arctan\left(\frac{b^*}{a^*}\right) \times \frac{180}{\pi} + 180, \text{ for } a^* < 0 \tag{2}$$

$$h^o = \arctan\left(\frac{b^*}{a^*}\right) \times \frac{180}{\pi} + 360, \text{ for } a^* > 0 \text{ and } b^* < 0 \tag{3}$$

The chroma (C^*) indicates the saturation of colour. This parameter can be calculated using Equation (4):

$$C^* = \left((a^*)^2 + (b^*)^2\right)^{\frac{1}{2}} \tag{4}$$

The total colour difference (ΔE^*_{ab}) takes into account the changes in L^*, a^*, and b^* that may occur between two samples. It can be calculated with Equation (5). In this work, this parameter was calculated between the white calibration plate and each sample. If $\Delta E^*_{ab} > 1$, then the colour difference should be visible to the naked eye.

$$\Delta E^*_{ab} = \left((\Delta L^*)^2 + (\Delta a^*)^2 + (\Delta b^*)^2\right)^{\frac{1}{2}} \tag{5}$$

The colourimeter was first calibrated against the white calibration plate, where $L^* = 94.6 \pm 0.03$, $a^* = -0.56 \pm 0.02$, and $b^* = 3.65 \pm 0.06$. Then, the film colour was measured five times against the white calibration plate.

2.7.3. Barrier Properties to UV-vis Radiation

Film samples were cut into rectangular sections (10 mm × 40 mm) and placed against quartz cuvettes' inside wall. A scan of the films' transmittance in the ultraviolet-visible (UV-vis) spectrum, ranging from 200 nm up to 800 nm, was obtained using a spectrophotometer (Cary 100 UV-Vis, Agilent Technologies, Santa Clara, CA, USA). The measurement was carried out in triplicate.

2.7.4. Water Vapour Permeability

The films' water vapour permeability (*WVP*) was determined gravimetrically based on the method used by Weng et al. [26] with slight modifications. Film triplicates were cut into circular samples and sealed with aluminium tape on top of cylindrical glass cups with 9 mL saturated solution of sodium chloride (a_w = 0.753). The films had a circular exposed area with a diameter of 40 mm. The glass cups were weighed and then placed in a desiccator equipped with a fan to promote air circulation inside and to minimize the resistance of mass transfer above the film. This desiccator contained a saturated solution of magnesium chloride (a_w = 0.328). Over the course of 9 h at regular time intervals, the temperature and relative humidity were monitored using a thermohygrometer (Vaisala HUMICAP® HM40, Helsinki, Finland), and the glass cups containing the films were weighed to measure the water vapour flux.

The water vapour permeability (*WVP*) was calculated with Equation (6), where N_w (mol/m^{2}s) represents the water vapour flux, δ (m) is the film thickness, and $\Delta P_{w,eff}$ (Pa) indicates the effective driving force, expressed as the water vapour pressure difference between both sides of the film:

$$WVP = \frac{N_w \times \delta}{\Delta P_{w.eff}} \tag{6}$$

The N_w was determined by dividing the slope of the plotted water loss of the glass cups vs. time (mol/s) by the area of the film exposed (m^2). The $\Delta P_{w,eff}$ was calculated using Equation (7) in which P_{w2} (Pa) represents the water partial pressure in contact with the film, and P_{w3} (Pa) represents the water partial pressure in the desiccator:

$$\Delta P_{w,eff} = P_{w2} - P_{w3} \tag{7}$$

The unknown value of P_{w2} was determined using Equation (8), taking into consideration that, at steady-state conditions, the N_w value was equal to the flux through the stagnate layer of air that separated the surface of the liquid from the inner surface of the film:

$$N_w = \frac{P}{RTz} D_{w-air} \; ln\left(\frac{P - P_{w2}}{P - P_{w1}}\right) \tag{8}$$

In this last equation, P (Pa) is the atmospheric pressure, R (J K^{-1}mol^{-1}) is the gas constant, T (K) is the mean temperature, z (m) is the distance from the film to the solution in the glass cup, $D_{w\text{-}air}$ (m^2/s) is the water vapour diffusion coefficient in air, and P_{w1} (Pa) is the water partial pressure in contact with the solution in the glass cup. This last parameter was obtained with Equation (9), where a_w represents the water activity of the saturated solution in the glass cups, and P_w^* (Pa) is the pure water vapour pressure calculated using Equation (10):

$$P_{w1} = a_w \times P_w^* \tag{9}$$

$$P_w^* = exp\left(23.2 - \frac{3816.4}{T - 46.1}\right) \tag{10}$$

Finally, P_{w3} was determined with Equation (11) using the mean value of RH (relative humidity):

$$\text{RH } (\%) = \frac{P_{w3}}{P_w^*} \times 100 \tag{11}$$

2.7.5. Gas Permeation Studies

The permeability of O_2 through the produced films was measured using the set-up illustrated in Figure 1. The set-up consisted of a feed compartment connected to a gas reservoir where the feed pressure was kept constant by using a back-pressure controller. The feed compartment was separated from the permeate compartment by a film, which was placed in a membrane module. The permeate compartment was connected to a vacuum pump, which was controlled externally by a valve.
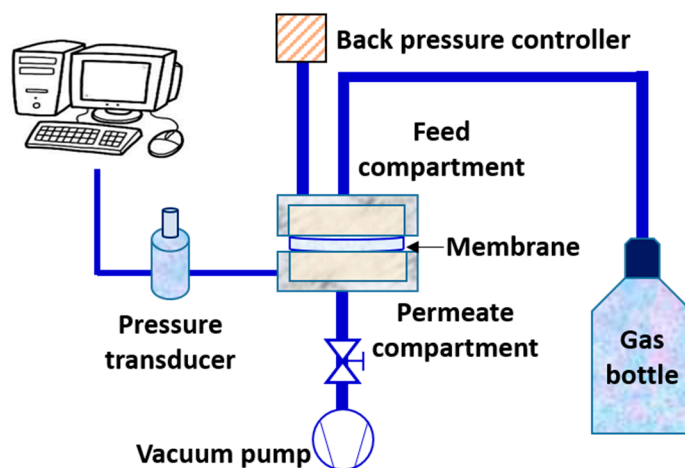

Figure 1. Schematic representation of the set-up used for gas permeability studies.

To evaluate the gas permeation, the film under study was placed within the membrane module, and the permeate compartment was initially placed under vacuum conditions to degas the membrane and to remove any trapped gases within the unit until the pressure was stable (~0 bar). Following this, the valve regulating the vacuum into the system was closed. O_2 was supplied into the system at a constant feed pressure of 1.05 bar, and the variation in pressure in the permeate compartment was monitored in real time.

The transport was defined using Equation (12), where J_{mol} (mol·m^{-2}·s^{-1}) is the molar flux (the ratio between the molar flow rate Q_{mol} (mol·s^{-1}) and the membrane area A (m^2)), P_{mol} (mol·m^{-1}·s^{-1}·Pa^{-1}) is the molar permeability, Δp (Pa) is the driving force calculated by the difference between the feed and permeate pressures, and δ (m) is the membrane thickness:

$$J_{mol} = \frac{P_{mol} \times \Delta p}{\delta} \tag{12}$$

The volumetric gas flow rate Q_{vol} (Pa·m^3·s^{-1}) and the corresponding molar flow rate Q_{mol} (mol·s^{-1}) are given by the equations below:

$$Q_{vol} = \frac{dp}{dt} \times V_{perm} \tag{13}$$

$$Q_{mol} = \frac{1}{RT} \times Q_{vol} \tag{14}$$

where T is the operating temperature (K). Subsequently, the molar permeability P was calculated with Equation (15):

$$Molar\ Permeability\ (P) = \frac{Q_{mol} \times \delta}{\Delta p \times A} \tag{15}$$

2.7.6. Moisture Content

The moisture content in a dry basis (MC, %) of the films, which were equilibrated beforehand in a desiccator at room temperature with a relative humidity of $55 \pm 5\%$ for 24 h, was determined. The film samples were first weighed (m_1, g) and then dried at 40 °C overnight. Then, they were stored in a silica gel desiccator at room temperature for 72 h. Lastly, the films were weighed once again (m_2, g), and the MC was calculated using Equation (16):

$$MC\ (\%) = \frac{m_1 - m_2}{m_1} \times 100 \tag{16}$$

2.7.7. Solubility

The solubility (S, %) of the films was measured following the procedure from Ferreira et al. [27] with minor adjustments. Film samples in triplicate were cut to a size of 10×10 mm and dried under the conditions described in Section 2.7.6 to obtain a dried sample mass (m_1, g). Then, the dried samples were immersed in 5 mL distilled water for 24 h at room temperature. Afterwards, the resulting solution was centrifugated at 5000 rpm for 5 min (Hermle Labortechnik Gmbh Z 383 K, Wehingen, Germany), and the liquid was discarded. The pellet was then dried at 40 °C for 24 h and weighed to obtain the final mass (m_2, g). The solubility was calculated using Equation (17):

$$S\ (\%) = \frac{m_1 - m_2}{m_1} \times 100 \tag{17}$$

2.7.8. Contact Angle Measurements

The static contact angle was obtained using the sessile drop method using a Drop Shape Analyser—DSA25 (KRÜSS, Hamburg, Germany) and Advance software to analyse the results. The measurements were performed at room temperature over the course of 5 s after a water drop was placed on the upper surface of the film, which was not in contact with the Teflon dish where the films were dried. For each film type, at least five measurements at different positions on the surfaces of the films were performed.

2.7.9. Antioxidant Activity by Ferric Reduction Antioxidant Power (FRAP) Method

The antioxidant activity of the films in triplicate was determined by the FRAP method. First, the FRAP reagent was prepared with 25 mL of acetate buffer (0.3 M, pH = 3.6), 2.5 mL of TPTZ (2.4.6-Tri(2-pyridyl)-1.3.5-triazine) solution (10 mM in HCL 40 mM), and 2.5 mL of ferric chloride (20 mM). Next, 270 μL of distilled water, 2.7 mL of FRAP reagent, and 2.21 ± 0.14 mg of film sample were added to a test tube, which was then homogenised in a vortex (RSLAB-6PRO, Auxilab S.L., Navarra, Spain) and incubated at 37 °C in a water bath (Precision, Thermo Scientific, USA) in the dark for 30 min. When this step was completed, the solutions were diluted at a proportion of 1:3, and the absorbance was measured at $\lambda = 595$ nm (Cary 100 UV-Vis, Agilent Technologies, Santa Clara, CA, USA). A standard curve with different concentrations of Trolox standard solution (ranging from 0 to 2.5×10^{-5} M) was used to determine the antioxidant activity expressed as Trolox equivalent antioxidant activity (TEAC) in μmol Trolox/mg film.

2.7.10. Mechanical Properties

Tensile tests were performed at room temperature using a texturometer (TA-XT-plus, Stable Micro System, Surrey, UK). Prior to the experiment, seven samples of each type of film were cut into rectangles (10 mm × 50 mm) and stored in a desiccator at room temperature with a relative humidity of 55% ± 5 for 72 h. Both ends of each sample were fixed with tensile grips and extended until rupture at a constant speed of 1 mm/s with an initial distance of 30 mm of film between the grips. Using the data of force exerted as a function of distance, the tensile stress at the break was calculated, as well as elongation at the break and Young's modulus.

The tensile stress at the break (σ, MPa) was calculated by dividing the maximum force (F, N) by the initial cross-sectional area of the sample (S, m^2) (Equation (18)). This element expressed the maximum load that the film could support during stretching without rupture:

$$\sigma = \frac{F}{S} \tag{18}$$

For elongation at the break (ε), Equation (19) was applied, where l_f (mm) is the final length of the film just before its tearing point, and l_i (mm) is the initial length of the film:

$$\varepsilon = \frac{l_f - l_i}{l_i} \tag{19}$$

The Young's modulus (E, MPa) was obtained from the slope of the linear correlation in the elastic deformation region of the stress–strain curve. This parameter indicated the resistance of the film to deformation.

2.7.11. Films' Morphology

The films' surface and cross-section morphologies were analysed with scanning electron microscopy (SEM). The film samples were placed on aluminium stubs using double-sided carbon tape and were sputter-coated with a thin Au/Pd film with a Quorum Technologies coater (Q150T ES). They were then analysed with a Thermo Fischer Scientific desktop scanning electron microscope (Phenom ProX G6) equipped with an energy dispersive spectroscopy (EDS) light element.

2.7.12. Statistical Analysis

In this work, Statistic 10.0 software (StatSoft Inc., Tulsa, OK, USA) was used to perform the analysis of variance (ANOVA), as well as a post hoc Tukey test ($p < 0.05$), in order to detect differences between the mean value of each property observed in the films.

3. Results and Discussion

3.1. Interfacial Tension

The interfacial tension results between each aqueous sample and oleic acid can be observed in Table 2. As expected, the interfacial tension values found in the samples without any surfactant (samples 1 and 4) were the highest. These values show that the presence of a surfactant was required to stabilise the studied emulsions. Furthermore, the interfacial tension value obtained in sample 4 decreased significantly in comparison with sample 1 since arabinoxylan, similar to other polysaccharides, has emulsion-stabilizing proprieties, as previously mentioned.

Table 2. Interfacial tension results (γ, mN/m) between each aqueous solution and oleic acid. Values in the same column followed by different superscript letters differ significantly ($p < 0.05$).

	Sample	γ (mN/m)
1.	Distilled water	13.32 $\pm$ 0.02 [f]
2.	2% Tween 20	1.41 $\pm$ 0.24 [a,b]
3.	5% Tween 20	1.02 $\pm$ 0.41 [a,c]
4.	AX 2% + Glycerol	4.36 $\pm$ 0.5 [e]
5.	AX 2%+ Glycerol + 0.05% Tween 20	2.41$\pm$ 0.32 [d]
6.	AX 2% + Glycerol + 0.1% Tween 20	1.49 $\pm$ 0.18 [b]
7.	AX 2% + Glycerol + 0.2% Tween 20	1.34 $\pm$ 0.22 [a,b]
8.	AX 2%+ Glycerol + 0.5% Tween 20	1.09 $\pm$ 0.16 [a,b,c]
9.	AX 2%+ Glycerol + 1% Tween 20	1.06 $\pm$ 0.27 [a,b,c]
10.	AX 2%+ Glycerol + 2% Tween 20	0.84 $\pm$ 0.13 [c]

In samples 2 and 3, the interfacial tension values dropped even further and were remarkably similar between them. This allowed the conclusion that 2% Tween 20 was sufficient to create a stable emulsion of oleic acid dispersed in an aqueous AX (2% w/w) solution. The addition of increasing concentrations of Tween 20 to the film-forming solutions (samples 5 to 10) resulted in a constant decrease in the interfacial tension values, which suggests that an increase in the surfactant concentration ensured a higher probability of forming a stable emulsion. Having these results in consideration and seeing that the interfacial tension value with 1% surfactant was already an extremely low value, a concentration of 1% of Tween 20 was selected for the films' formulation.
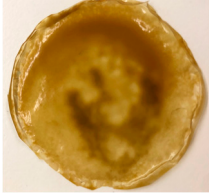
3.2. Visual Appearance of Films

The images captured of the films after they were dried and peeled are presented in Table 3. All the films were easy to peel from the casting container and easy to handle due to their flexible and malleable structures. They were brownish-yellow in colour, which is characteristic of the corn fibre from where the arabinoxylan was extracted.

Both the control and the multilayer films (samples 1 and 6, respectively, Table 3) had smooth, intact, uniform, and homogeneous surfaces. However, the multilayer film appeared to be more opaque and mattified than the control film due to the beeswax coating. This coating uniformly covered the whole film.

The addition of oleic acid (samples 2 to 5, Table 3) resulted in films with a darker colour and a nonuniform and heterogeneous structure from naked-eye observation. As the concentration of the oil increased, the films revealed a glossier and darker appearance with a higher degree of heterogeneity. These results may have occurred due to poor oil droplet distribution throughout the film matrix. The migration of oil aggregates or droplets throughout the films' networks may have occurred during the drying step, or even some flocculation and creaming, which could lead to some structure irregularities.

Table 3. Visual appearance of composite films.

Sample	Image	Sample	Image
1. AX + Glycerol (control)		4. AX + Glycerol + Tween 20 + 0.75% OA	
2. AX + Glycerol + Tween 20 + 0.25% OA		5. AX + Glycerol + Tween 20 + 1% OA	
3. AX + Glycerol + Tween 20 + 0.50% OA		6. AX + Glycerol + Beeswax coating	

Furthermore, poor oil droplet distribution resulted in films with uneven thicknesses and different shades of colour throughout the film itself. The areas of the film where the oil accumulated were thicker, denser, and darker in colour, whereas the remaining areas were thinner and lighter in colour with smoother surfaces.

3.2.1. Thickness

The films' thicknesses are presented in Table 4. The control film (sample 1, Table 4) was the thinnest and had the most homogeneous thickness. Comparing this sample to the arabinoxylan-based films found in the literature, Weng et al. reported a similar result for a film with the same formulation as this work (101 ± 12 µm) [26], while Péroval et al. reached a slightly lower value, 90.8 ± 6.6 µm, as their arabinoxylan film had some differences in composition when compared to the control film sample [24].

Table 4. Thicknesses of all the film samples. Values in the same column followed by different superscript letters differ significantly ($p < 0.05$).

Sample	Thickness (µm)
1. AX + Glycerol (control)	101 ± 12.3 [a]
2. AX + Glycerol + Tween 20 + 0.25% OA	156.4 ± 23.9 [b]
3. AX + Glycerol + Tween 20 + 0.5% OA	213.2 ± 45.5 [d]
4. AX + Glycerol + Tween 20 + 0.75% OA	302.1 ± 30.1 [c]
5. AX + Glycerol + Tween 20 + 1% OA	301.6 ± 50.3 [c]
6. AX + Glycerol + Beeswax coating	105.8 ± 25 [a]
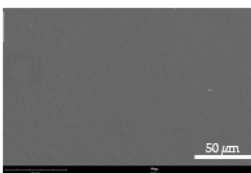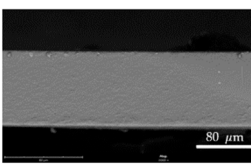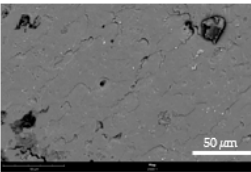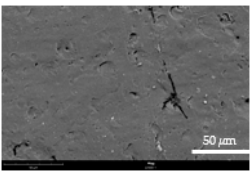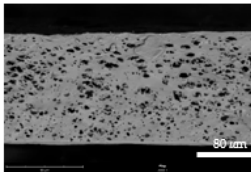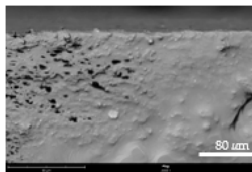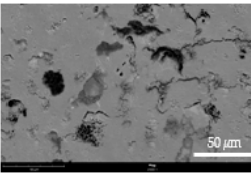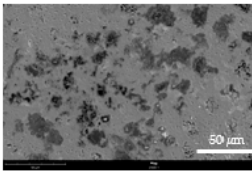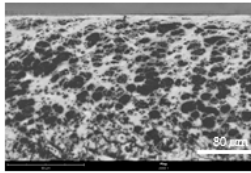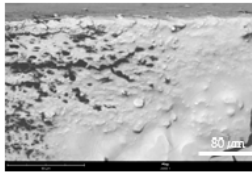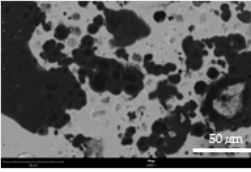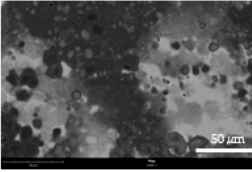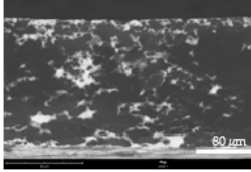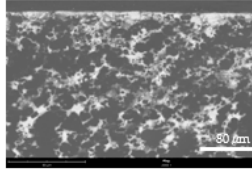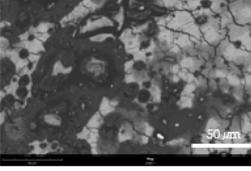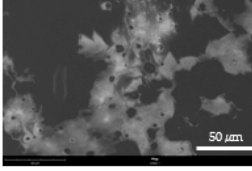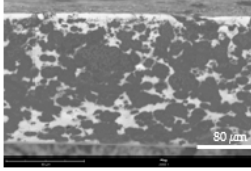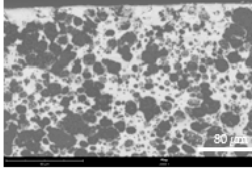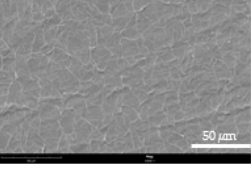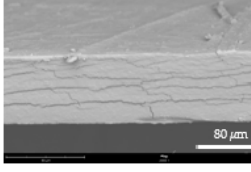
As stated before, the addition of oil (samples 2 to 5, Table 4) produced films with uneven thicknesses. Hence, their standard deviations were superior. Additionally, the increase in oleic acid concentration was followed by an increase in the films' thicknesses. Aguirre-Loredo et al. also observed that the thickness of chitosan-based films was influenced by the addition of oleic acid, rising as the amount of oleic acid incorporated increased [28].

In addition, composite films made of cellulose sulfate with oleic acid were also reported to have an increase in their thicknesses with the introduction of this lipid [29]. Lastly, the film coated in the beeswax solution (sample 6, Table 4) exhibited a similar thickness to the control film sample, showing no statistically significant differences between them ($p > 0.05$). This indicates that the beeswax coating was thin and hardly detectable. Velickova et al. also reported this occurrence in chitosan films coated on both surfaces with a beeswax solution, which contained a quarter of the amount of beeswax used in this work [17].

3.2.2. Films Morphology

The films' surface and cross-section morphologies, analysed by scanning electron microscopy (SEM), are shown in Table 5.

Table 5. SEM images of the surfaces and cross-sections of all the film samples.

Sample	Surface		Cross-Section	
	Homogeneous Areas of the Film	Heterogeneous Areas of the Film	Homogeneous Areas of the Film	Heterogeneous Areas of the Film
1. AX + Glycerol (control)				
2. AX + Glycerol + Tween 20 + 0.25% OA				
3. AX + Glycerol + Tween 20 + 0.5% OA				
4. AX + Glycerol + Tween 20 + 0.75% OA				
5. AX + Glycerol + Tween 20 + 1% OA				
6. AX + Glycerol + Beeswax coating				

Both the surfaces and cross-sections were studied for homogeneous and heterogenous areas of the emulsified films detected visually (Table 3). It is possible to observe that the control film showed a smooth and uniform surface and cross-section without any visible cracks. However, the addition of oleic acid changed considerably the microstructure of the

arabinoxylan films resulting, in a heterogeneous structure with several dark spots attributed to the oleic acid phase. In fact, both the aqueous and oil phases were well-distinguished, both on the homogeneous and heterogeneous areas of the films, increasing the dark areas as the content of oleic acid was higher. For lower oleic acid incorporations (0.25% and 0.50% OA), the oil droplets were well-distributed within the film cross-sections. However, for higher oil contents (0.75% and 1.0% OA), oil droplet coalescence was observed in the cross-section pictures, forming large oil areas within the AX matrix.

The multilayer film's surface showed a microstructure compatible with the coating formed by the solidification of beeswax upon ethanol evaporation during the coating process. On the other hand, in the cross-section pictures, small cracks were detected that were not observed in the control film of AX. It was envisaged that these cracks were formed during the coating process, which implied immersion in an ethanolic beeswax solution at 70 °C.

3.2.3. Colour

The colour measurement results are summarised in Table 6. Both the control and the multilayer films (samples 1 and 6) showed similar values of lightness, chromaticity coordinates, and chroma, which suggests that the beeswax coating did not affect the film colour.

Table 6. Values of lightness (L^*), chromaticity coordinates (a^*, b^*), the calculated hue ($h°$), chroma (C^*), and composite colour difference (ΔE^*_{ab}) for all the films samples. Values in the same column followed by different superscript letters differ significantly ($p < 0.05$).

	Sample	L^*	a^*	b^*	$h°$	C^*	ΔE^*_{ab}
1.	AX + Glycerol (control)	77.17 ± 1.15 [b]	1,63 ± 0.43 [a]	40.52 ± 1.29 [a]	88.03 ± 0.83 [a]	40.58 ± 1.28 [b,c]	41.31 ± 1.43 [a]
2.	AX + Glycerol + Tween 20 + 0.25% OA	73.67 ± 1.59 [c]	2.23 ± 0.73 [a]	39.81 ± 1.02 [a,c]	86.8 ± 1 [a]	39.89 ± 1.03 [a,b,c]	42.1 ± 1.58 [a]
3.	AX + Glycerol + Tween 20 + 0.5% OA	69.92 ± 1.54 [a]	3.93 ± 0.45 [b]	38.63 ± 0.63 [b,c]	84.02 ± 0.85 [c]	38.84 ± 0.62 [a,b]	43.27 ± 1 [a]
4.	AX + Glycerol + Tween 20 + 0.75% OA	69.55 ± 2.14 [a]	4.56 ± 1.05 [b]	37.68 ± 0.74 [b]	87.71 ± 1.83 [b]	38.49 ± 0.89 [a]	42.8 ± 1.9 [a]
5.	AX + Glycerol + Tween 20 + 1% OA	69.33 ± 1.4 [a]	4.22 ± 0.34 [b]	32.82 ± 0.78 [d]	82.72 ± 0.67 [b,c]	33.43 ± 0.77 [d]	39.09 ± 0.82 [a]
6.	AX + Glycerol + Beeswax coating	76.64 ± 1.36 [b]	2.21 ± 0.63 [a]	40.36 ± 1.48 [a]	87.12 ± 1 [a]	40.41 ± 1.82 [c]	40.35 ± 1.86 [a]

The films to which oleic acid was added (samples 2 to 5, Table 6) exhibited a decrease in the value of L^*, which is in agreement with the darker colour observed in Section 3.2. Moreover, these films showed a higher a^* value in comparison with the control and the multilayer films, which indicated a colour-shift towards red, and a lower b^* value, which entailed a colour-shift further from yellow. In addition, the addition of oleic acid resulted in a decrease in the C^* value, which is to say, a decrease in the films' colour saturation.

The hue values calculated for all the samples, ranging from 82 to 88°, did not change substantially between all the samples (Table 6). This interval corresponds to a yellowish colour, which was the colour observed in the films' pictures (Table 3).

The composite colour difference calculated between the film samples and the white calibration plate showed no statistically significant differences between all the samples ($p > 0.05$), which suggests that all the samples were quite similar in colour when compared to the white calibration plate (Table 6).

When comparing to results obtained previously for arabinoxylan-based films, Weng et al. observed similar values for a control film sample (sample 1, Table 5) regarding the parameters of $h°$ and C^*, which were 89.33 ± 0.57 and 46.86 ± 1.91, respectively [26]. The resemblance in the results is most likely due to the similarity in the film formulation and composition. In addition, Moreirinha et al. reported different values of lightness and

chromaticity coordinates for films made of arabinoxylan extracted from brewer's spent grain (BSG): an *L** value of 44.19 ± 0.15, an *a** value of 0.04 ± 0.02, and a *b** value of 6.11 ± 0.21 [30]. These results indicate that the arabinoxylan films produced in this work were darker in colour with a more intense yellow shade.

There were no reported data found regarding the optical properties of biodegradable films made from arabinoxylan with the addition of oleic acid or another lipid or coated with beeswax in order to compare the results obtained.

3.2.4. Barrier to UV-vis Radiation

A scan of the films' transmittance (T, %) in the ultraviolet-visible (UV-vis) spectrum, ranging from 200 nm up to 800 nm, can be observed in Figure 2. Although consumers may prefer and willingly accept biodegradable films with a more transparent and less opaque appearance, the capability of the packaging material to act as a barrier against UV-vis light is more important and is considered an added value in terms of the photostability of specific foods [31].
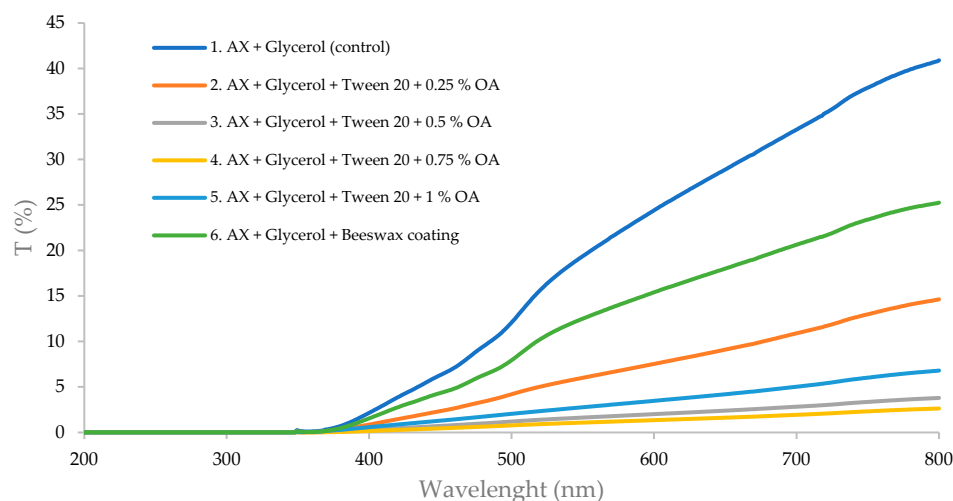

Figure 2. Transmittance (T, %) in the ultraviolet-visible spectrum, ranging from 200 nm up to 800 nm, of all film samples.

The spectra of all the film samples revealed transmittance values very close to 0% in the UV region (200–400 nm) (Figure 2). This indicates that all the films presented UV-blocking properties, which makes them excellent barriers against UV radiation, aiding in the prevention of photo-oxidation in light-sensitive foods and extending their shelf lives.

In the visible region, as the wavelength increased, all the film samples showed an increase in their transmittance values. The control film sample (sample 1, Figure 2) reached the highest value of transmittance, around 41% at 800 nm, while the others reached lower values (samples 2 to 6, Figure 2), which suggests that visible light passed more easily through the control film than through the multilayer film and, lastly, through the emulsified films. This is to say that the heterogenicity that oleic acid originated in the films' matrices resulted in a higher absorption capacity in the visible region.

In another study, Moreirinha et al. [30] measured the UV-vis transmittance spectrum of arabinoxylan-based films, which showed higher transmittance values in both the visible region (around 57% at 700 nm) and UV-A region (around 37% at 400 nm) in comparison with our control film sample (sample 1, Figure 2). In the UV-B and UV-C regions, the transmittance values (near 0%) were similar to the results obtained in this work.

Unlike arabinoxylan, other polysaccharides, such as chitosan, show very weak UV-blocking properties and higher transmittance values in the visible region, which is probably due to the appearance of the films, as they are glossy and transparent [31].

The films obtained in this work presented a higher capacity in blocking the most damaging light wavelengths and, therefore, would prevent the formation of toxic substances,

off-odours and flavours; avoid colour loss of food; and inhibit the photo-oxidation of lipids in food products.

3.2.5. Water Vapour Permeability

The water vapour permeability (*WVP*) values are exhibited in Table 7 (driving force of 75/33%, relative humidity (RH) (%)). Considering the hydrophilic nature of the polysaccharide arabinoxylan and the heterogeneity of the films with oleic acid, high *WVP* values were expected for samples 1 to 5. As the concentration of oleic acid increased (samples 2 to 5, Table 7), the films' *WVP* values increased, except in sample 4, which indicates that these films performed worse in preventing the transfer of moisture than the control film (sample 1, Table 7). This can be justified by the uneven lipid distribution, which resulted in two types of regions scattered throughout the film: denser and more resistant areas in which the oleic acid accumulated and thinner and more fragile patches through which the water vapour could easily be transferred. In addition, the increase in water vapour permeability could also be attributed to random irregularities in the film structure that appeared during the drying process, such as small voids and channellings, in the polysaccharide–lipid interface that enabled the diffusion of water molecules. The water that enters through films acts not only as a diffusion species but also as a plasticiser, which loosens the polymeric matrix, increasing the intermolecular spaces and, consequently, facilitating water vapour transport [32].

Table 7. Water vapour permeability (*WVP*, 10^{-11} mol/m·s·Pa) of all the film samples. Values in the same column followed by different superscript letters differ significantly ($p < 0.05$).

	Sample	*WVP* (10^{-11} mol·m·s·Pa)
1.	AX + Glycerol (control)	5.18 ± 0.47 [b]
2.	AX + Glycerol + Tween 20 + 0.25% OA	6.55 ± 0.66 [b]
3.	AX + Glycerol + Tween 20 + 0.5% OA	13.44 ± 2.40 [a]
4.	AX + Glycerol + Tween 20 + 0.75% OA	11.65 ± 1.73 [a]
5.	AX + Glycerol + Tween 20 + 1% OA	14.41 ± 1.84 [a]
6.	AX + Glycerol + Beeswax coating	0.58 ± 0.06 [c]

The multilayer film (sample 6, Table 7) showed the lowest value of *WVP*. This was foreseen since the additional uniform lipid layers should improve the moisture barrier properties of the control film. In addition, it is known that edible waxes such as beeswax are considerably more resistant to moisture transport than most liquid lipids [33]. As this film held the lowest water vapour permeability value, it would be the most efficient for reducing the transfer of moisture between the food product and the surrounding atmosphere, which is desirable for prolonging a product's shelf life.

Compared with other results found in the literature, Weng et al. reached a lower *WVP* value of $(2.62 \pm 0.96) \times 10^{-11}$ mol/m·s·Pa for an arabinoxylan film with the same formulation and similar thickness as the control film sample, but with a lower driving force (53/33%, RH (%)) [26]. In another study, Péroval et al. obtained a lower *WVP* value of $(0.98 \pm 0.03) \times 10^{-11}$ mol/m·s·Pa for an arabinoxylan film with 15% (*w/w*, AX basis) glycerol and a driving force of 84/22%, RH (%) [24]. These dissimilarities can be explained by differences in the driving forces, in the amounts of plasticiser, in the compositions of the arabinoxylan extract due to different methods of extraction and purification, or distinctive casting and drying conditions that influenced the structures of the resulting films.

Arabinoxylan-based films with 15% (*w/w*, AX basis) glycerol and fatty acids or oils (palmitic acid, stearic acid, triolein, or hydrogenated palm oil) showed a decrease in the water vapour permeability value after lipid incorporation, reporting the lowest value with triolein (driving force of 84/22%, RH (%)) [24]. Chen et al. also reported a decrease in

the water vapour permeability of cellulose-sulfate-based films with 15% (*w/w*, cellulose sulphate basis) glycerol after the addition of oleic acid [29].

As for the multilayer film, Velickova et al. also reported a decrease in the water vapour permeability value from a monolayer to a multilayer chitosan film (driving force of 90/44%, RH (%)) [33]. Comparable results of improved moisture barrier properties when applying lipid layers were reported by Weller et al., who obtained bilayer films from zein with sorghum wax and carnauba wax [34].

When comparing the values of water vapour permeability to those of other polysaccharide-based films, such as pectin ((5.13 ± 0.19) $\times 10^{-11}$ mol/m·s·Pa) with a driving force of 100/53%, RH (%)) [32], or chitosan ((4.13 ± 0.13) $\times 10^{-11}$ mol/m·s·Pa) with a driving force of 77/23%, RH (%)) [27], it is possible to observe that this work's arabinoxylan control film showed a higher *WVP* value.

The synthetic polymer LDPE, frequently used in the plastic-packaging industry, has a significantly lower value of *WVP* than any of the films presented in Table 7 of 0.01×10^{-11} mol/m·s·Pa with a driving force of 84/22%, RH (%) (thickness of 25 µm) [24].

3.2.6. Gas Permeation Studies

It is essential to study the gas permeability properties of a film for applications in the food-packaging industry to ensure the lowered degradation of packaged food. Polysaccharide-based films are known to have excellent gas barrier properties to O_2 at low relative humidity conditions, exhibiting a reduction in the loss of aroma compounds and prevention of the penetration of solvents, which may result in the toxicity of food [35,36]. The values obtained for the permeability of O_2 in the present study are presented in Figure 3.
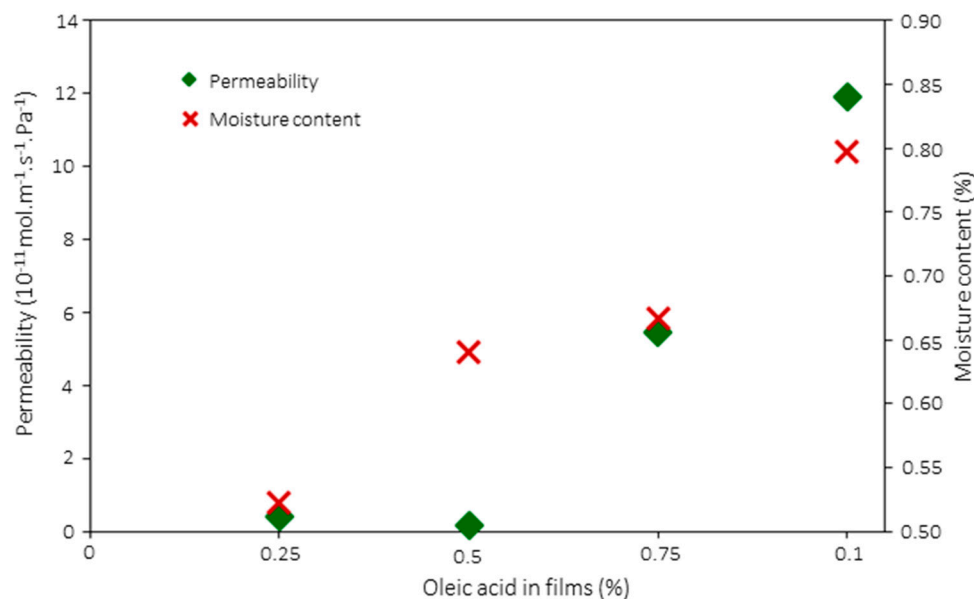

Figure 3. Effect of oleic acid and moisture content in films on their permeability to O_2. Standard deviation of the presented data was <10%.

The permeability of O_2 through the control film was 2.12×10^{-11} mol·m^{-1}·s^{-1}·Pa^{-1}, while the permeability of O_2 through the film sample coated in beeswax was lower at 3.28×10^{-12} mol·m^{-1}·s^{-1}·Pa^{-1}. When comparing the films containing oleic acid, it was observed that there was an increase in the permeability of O_2 as the percentage of oleic acid increased, as depicted in Figure 3. The O_2 permeability increased from 1.58×10^{-12} mol·m^{-1}·s^{-1}·Pa^{-1} to 1.19×10^{-10} mol·m^{-1}·s^{-1}·Pa^{-1} for the films containing 0.5% and 1% oleic acid, respectively. A trend of increase in O_2 permeability with the percentage of oleic acid was also reported by Aguirre-Loredo et al. in chitosan-based films containing oleic acid [28]. In the present study, it was also observed that there was an increase in the moisture content of the films with the increase in oleic acid percentage

(Table 8). Therefore, the increase in gas permeability could also be linked to the increase in the moisture content of the films, as has been reported in the literature for hydrophilic films made of polysaccharides [28,37].

Table 8. Moisture content (MC, %) of all the film samples. Values in the same column followed by different superscript letters differ significantly ($p < 0.05$).

Sample	MC (%)
1. AX + Glycerol (control)	7.37 ± 0.40 [b,c]
2. AX + Glycerol + Tween 20 + 0.25% OA	5.23 ± 0.02 [d]
3. AX + Glycerol + Tween 20 + 0.5% OA	6.41 ± 0.4 [a]
4. AX + Glycerol + Tween 20 + 0.75% OA	6.67 ± 0.63 [a,b]
5. AX + Glycerol + Tween 20 + 1% OA	7.97 ± 0.58 [c]
6. AX + Glycerol + Beeswax coating	10.9 ± 0.06 [e]

There are not many studies reporting the permeability of O_2 through biopolymer films when compared to those of water vapour permeability. However, the literature does state that the ability of biopolymer films to be potential barriers of gases is highly dependent on the microstructure and the water content of the film. Gontard et al. ascribed the increase in gas permeation to the plasticization effect on the amorphous nature of the backbone of the biopolymer due to water molecules. The interaction of hydrophilic groups with water molecules disrupted the hydrogen bonding. As a result, additional sites for oxygen dissolution were created while causing an increase in the mobility of the molecules within the polymer [37]. Even so, the O_2 permeability observed in this work for the control film was higher than that usually referred to for polysaccharide films. In addition to the water-plasticizing effect, our presented films may not be completely dense, with micro- or nano-fissures that were not detected in the morphology studies by SEM.

3.2.7. Moisture Content

The moisture content (MC) results are presented in Table 8. The incorporation of oleic acid in the films' formulation should cause a barrier between water and the hydrophilic groups of the arabinoxylan chains, leading to a decrease in the availability of hydroxyl groups and limiting their interactions with water through hydrogen bonds. This chain of events should result in a reduction in the films' moisture contents [38]. Even though the samples with 0.25, 0.5, and 0.75% oleic acid (samples 2, 3, and 4, Table 8) showed lower moisture content values than the control film sample (sample 1, Table 8), there was still a tendency of increasing water content as the oleic acid concentration increased. Once again, these results were most likely due to the heterogeneous network of the emulsified films that resulted in free hydroxyl groups available to interact with the water molecules. Thus, both the affinity of the polysaccharide towards the water molecules and the arabinoxylan matrix's water uptake capacity increased.

The multilayer film revealed the highest value of moisture content: 10.9% (sample 6, Table 8). This occurrence was not expected, as beeswax is known to have an extremely low water uptake capacity due to its high hydrophobic nature. Nevertheless, this may be attributed to water entrapped in small pores between the arabinoxylan and the beeswax layers upon the films' immersion in the beeswax solution.

It is difficult to compare the moisture content with other values reported in the literature since the amount of bound water is extremely dependent on film composition and the time and temperature of drying [31]. This work had an oven drying temperature significantly lower than most of the reported studies. Ghasemlou et al. reported a decrease in the moisture content value of emulsified kefiran films with the increase in the concentration of oleic acid, from 17.95% without oleic acid to 12.36% with 0.7% (*w/w*) oleic acid (oven drying temperature of 103 ± 2 °C) [38].

3.2.8. Solubility in Water

The films' solubility in water was evaluated in order to examine whether the addition of oleic acid through emulsion or the coating of the film surfaces with a solution of beeswax would decrease their water solubility. All the film samples were dissolved in water after being immersed in distilled water for 24 h.

These results are most likely due to the hydrophilic nature of arabinoxylan and the films' appearance and compositions. Even though the multilayer films were more water-resistant, the water still managed to transfer through the beeswax layers, reaching the arabinoxylan film and dissolving it once again. It is important to reference that, after the first drying step of the method used to determine water solubility, the multilayer film samples became brittle, which perhaps resulted in small cracks in the wax not observable to the naked eye. These cracks could be the entryway that enabled the water to enter the polymer matrix, thus completely dissolving the multilayer film.

Water solubility is an important parameter that indicates a film's resistance or tolerance to water and dictates its biodegradability. Highly soluble films can be seen as unfavourable in high relative humidity environments and high-moisture food products during storage [28]. For these particular conditions, the films produced in this work showed signs that they would not be suitable. Other biodegradable films based on arabinoxylan have reported similar value findings. Arabinoxylan films with the same formulation as this work obtained a relatively high value of solubility in water of 87 ± 10% [26]. However, films from other polysaccharides, such as pectin films, presented a very low water solubility value of about 19% [35]. In addition, FucoPol and chitosan films obtained intermediate values of water solubility of 47.5 ± 5.2% and 30.5 ± 0.5%, respectively [27]. Nevertheless, films based on brea gum also reported complete dissolution in water [35].

3.2.9. Contact Angle Measurements

The static water contact angle (θ) results are shown in Table 9. The films with oleic acid showed a drastic decrease in the contact angle value to 36.97 ± 1.87° with 0.25% OA and around 49° with 0.5, 0.75, and 1% OA (samples 2 to 5, Table 9) in comparison with that of the control film (82.87°). This suggests that the emulsified films' surfaces were more hydrophilic and had a higher affinity for water than the control film's surface. However, it is more likely attributed to the heterogeneity and irregularities found in the emulsified films' matrices, playing a key role in dictating irregular surface properties with increased roughness and, eventually, leading to an easier dispersion of the water droplet, overcoming the hydrophobic effect of oleic acid. This simultaneous effect of chemical composition and surface roughness on wettability was studied by Yu et al. for artificial sandstones [39]. In addition, the deposited water droplet rapidly permeated through the film's matrix after 30 s.

Table 9. Static water contact angle (θ, °) values of all the film samples. Values in the same column followed by different superscript letters differ significantly ($p < 0.05$).

	Sample	θ (°)
1.	AX + Glycerol (control)	82.87 ± 5.16 [c]
2.	AX + Glycerol + Tween 20 + 0.25% OA	36.97 ± 1.87 [b]
3.	AX + Glycerol + Tween 20 + 0.5% OA	48.62 ± 6.57 [a]
4.	AX + Glycerol + Tween 20 + 0.75% OA	49.17 ± 1.9 [a]
5.	AX + Glycerol + Tween 20 + 1% OA	48.22 ± 2.52 [a]
6.	AX + Glycerol + Beeswax coating	92.43 ± 3.92 [d]

In the case of the multilayer film (sample 6, Table 9), the contact angle value was the highest when compared to all the films tested. Since the $\theta > 90°$, it was possible to assume that this film's surface has a low wetting tendency. This is most likely due to the added beeswax layers, which granted the control film's surfaces enhanced hydrophobic

properties. Unlike the other film samples, the water drop placed on top of the multilayer film maintained its shape for a longer time period and permeated through the film's matrix at a slower pace.

A study with arabinoxylan-based films with 15% (*w/w*, AX basis) glycerol reached a water contact angle value slightly lower than the control film in this work: 70.8 ± 5.1° [24]. This observation is most likely due to the difference in the amount of plasticiser added. Additionally, the same study also reported the same occurrence as the results obtained in the present work since the addition of a lipid compound (palmitic acid (64 ± 4.6°), stearic acid (68.6 ± 3.6°) or triolein (39 ± 8.5°) decreased the water contact angle; however, the addition of hydrogenated palm oil improved the film's surface hydrophobicity, as the contact angle increased to 94.4 ± 2.1° [24].

A similar water contact angle value to the control film sample was reported by Slavutsky et al. for pectin-based films (78.26 ± 4.91°) [35]. Other polysaccharides, such as chitosan and cellulose sulphate, revealed lower water contact angles than the arabinoxylan control film of 58.1 ± 5° [27] and 64.2° [29], respectively, which indicates that these polysaccharide films had more hydrophilic surfaces.

Contrary to this work, emulsified cellulose sulphate films with 0.5% (*w/w*) oleic acid revealed an increase in the water contact angle value of the films once the oil was added from 64.2° to 94° [29]. Furthermore, Ghasemlou et al. reported the same event for kefiran films after the incorporation of oleic acid [38,40]. Commercial plastic films, particularly LDPE films, showed a higher water contact angle value of 100.7 ± 11.4° similar to the multilayer film in this work [24].

3.2.10. Antioxidant Activity by Ferric Reduction Antioxidant Power (FRAP) Method

The antioxidant activity results determined by the FRAP method are exhibited in Table 10. The presence of some phenolic compounds in the arabinoxylan extract, namely ferulic acid, is responsible for its antioxidant activity. These compounds were released during the alkaline extraction of arabinoxylan from corn fibre and remained in the extract after it was purified.

Table 10. Antioxidant activity (10^{-5} mmol Trolox/mg film) of all the film samples. Values in the same column followed by different superscript letters differ significantly ($p < 0.05$).

Sample	Antioxidant Activity (10^{-5} mmol Trolox/mg Film)
1. AX + Glycerol (control)	5.87 ± 0.33 [b]
2. AX + Glycerol + Tween 20 + 0.25% OA	3.87 ± 0.35 [a]
3. AX + Glycerol + Tween 20 + 0.5% OA	3.84 ± 0.29 [a]
4. AX + Glycerol + Tween 20 + 0.75% OA	3.29 ± 0.25 [a]
5. AX + Glycerol + Tween 20 + 1% OA	3.27 ± 0.13 [a]
6. AX + Glycerol + Beeswax coating	5.33 ± 0.24 [b]

The control film sample revealed the highest value of antioxidant activity, (5.87 ± 0.33) × 10^{-5} mmol Trolox/mg film (sample 1, Table 10). A previous study in which the arabinoxylan film had the same formulation and composition as our control film showed antioxidant activity of (4.15 ± 0.46) × 10^{-5} mmol Trolox/mg film [26]. The discrepancy in these results may be due to the high variability in the composition of purified arabinoxylan extract among different batches produced, more specifically, regarding the amount of ferulic acid and other phenolic compounds present.

The addition of oleic acid resulted in a significant decrease in the antioxidant activity as the oleic acid concentration was increased (samples 2 to 5, Table 10). This is most likely due to the uneven lipid distribution throughout the film's matrix that may have affected the amount and the dispersion of the phenolic compounds, as some areas of the film revealed

different physical and structural features. In addition to that, the mass of active substances per mass of film decreased when introducing oleic acid in the film matrix, which may have decreased the antioxidant activity expressed in the film weight basis.

3.2.11. Mechanical Properties

The mechanical performances of all the film samples were assessed by tensile tests, during which the stress–strain curves were obtained in order to determine the tensile stress at the break (σ), the elongation at the break (ε), and Young's modulus (E). The results are presented in Table 11. It is important to mention that all the multilayer film replicas always worked as a whole system, showing good adhesion between the three layers.

Table 11. Thickness (μm), tensile stress at break (σ, MPa), elongation at break (ε), and Young's modulus (E, MPa) of all film samples. Values in the same column followed by different superscript letters differ significantly ($p < 0.05$).

	Sample	Thickness (μm)	σ (MPa)	ε	E (MPa)
1.	AX + Glycerol (control)	101 ± 12.3 [a]	1.67 ± 0.47 [b]	4.77 ± 1.04 [c]	42.06 ± 9.54 [c]
2.	AX + Glycerol + Tween 20 + 0.25% OA	156.4 ± 23.9 [b]	1.91 ± 0.28 [b]	1.24 ± 0.27 [a]	2.24 ± 0.38 [a]
3.	AX + Glycerol + Tween 20 + 0.5% OA	213.2 ± 45.5 [d]	0.29 ± 0.07 [a]	1.69 ± 0.48 [a]	0.78 ± 0.3 [a]
4.	AX + Glycerol + Tween 20 + 0.75% OA	302.1 ± 30.1 [c]	0.15 ± 0.08 [a]	1.21 ± 0.28 [a]	0.4 ± 0.15 [a]
5.	AX + Glycerol + Tween 20 + 1% OA	301.6 ± 50.3 [c]	3.41×10^{-4} ± 9.53×10^{-5} [a]	1.08 ± 0.11 [a,b]	6.03×10^{-4} ± 1.68×10^{-4} [a]
6.	AX + Glycerol + Beeswax coating	105.8 ± 25 [a]	4.11 ± 0.63 [c]	0.62 ± 0.11 [b]	15.96 ± 1.96 [b]

The control film sample showed a tensile stress value of 1.67 ± 0.47 MPa (sample 1, Table 11); however, after the addition of oleic acid, the films' tensile stresses decreased, except for the film sample with 0.25% OA. The decrease in the tensile stress value with the incorporation of oleic acid indicates that the emulsified films withstood less stress while being stretched before breaking, which is most likely due to the increasing oil areas within the AX matrix observed by SEM (Table 5), which were large discontinuities imparting less strength to the overall film structure (samples 2 to 5, Table 11). On the other hand, the multilayer film sample revealed the highest value of tensile stress (4.11 ± 0.63 MPa), which indicates that coating both surfaces of the film with beeswax made it more resistant to deformation (sample 6, Table 11).

The elongation at the break showed the highest value for the control film sample, 4.77 ± 9.54 (sample 1, Table 11). Even though the emulsified and the multilayer films were still flexible and bendable without breaking, they were not as deformable, which resulted in a decrease in the elongation at break value (samples 2 to 6, Table 11). In the case of the emulsified films, this occurrence may be due to the increase in oil areas with poor interactions with the polar polymer molecules. This may have weakened the emulsified films' matrices, which triggered earlier tearing. For the multilayer film, which presented the lowest value of elongation at the break (0.62 ± 0.11), the extra layers of beeswax made the film stiffer, restraining its extension when pulled by the tensile grips. This led to a rapid fracture without any noticeable change in its length.

The control film sample showed the highest value of Young's modulus (42.06 ± 9.54 MPa), which indicates that this film was more resistant to being deformed elastically when stretched (sample 1, Table 11). After that was the multilayer film (sample 6, Table 11) and, lastly, the emulsified films (samples 2 to 5, Table 11), which means that these films needed less stress to create the same amount of strain. Once again, the results for the emulsified films are most possibly due to their biphasic structure introduced by the oil phase.

Péroval et al. studied the effects that different lipids (palmitic acid, stearic acid, triolein, and hydrogenated palm oil (OK35)) had on arabinoxylan films with 15 % (w/w AX basis) glycerol. An arabinoxylan film without any lipids showed higher values of tensile stress,

elongation at the break, and Young's modulus than the arabinoxylan control film of present work. The results obtained may be due to a difference in the amount of glycerol added since plasticisers interfere with arabinoxylan chains, decreasing the intermolecular forces, softening the film's structure, and increasing the polymer mobility. As in the present work, the addition of oil, whether it be palmitic acid, stearic acid, triolein, or OK35, decreased the three mechanical parameters, except the elongation at the break, for the arabinoxylan film with triolein [24].

Previous studies with biodegradable films made from other polysaccharides, such as pectin and chitosan, have also shown higher values of tensile stress, elongation at the break, and Young's modulus compared to the present work [20,30].

The mechanical properties of films made from synthetic polymers, namely PP, HDPE, and LDPE, are much greater than the results obtained for the films tested in this work, which suggests that they are still far from achieving the excellent mechanical performance of synthetic polymers [22,33].

4. Conclusions

Current environmental concerns urge the need to find better and viable alternatives to the currently used food-packaging materials. To face this challenge, this work contributed to the development of composite films based on arabinoxylan-oleic acid emulsions and arabinoxylan films with beeswax coatings (multilayer structure). Despite being soluble in water, both types of films presented suitable mechanical properties to be handled and to produce flexible packages. In addition, multilayer films showed higher barriers to water vapour, oxygen, and UV-vis radiation than the emulsion-based ones. Multilayer films also presented enhanced surface hydrophobicity. Although the production of these films on a large scale is not as easy as the production of petrochemical-based ones, from the results obtained, a good potential of the developed arabinoxylan films is envisaged for producing flexible packages for food products with low water contents (e.g., several types of nuts).

References

1. National Geographic. Eat Your Food, and the Package Too. Available online: https://www.nationalgeographic.com/environment/future-of-food/food-packaging-plastics-recycle-solutions/ (accessed on 8 October 2020).
2. Plastics Europe. Plastics—The Facts. 2019. Available online: https://plasticseurope.org/knowledge-hub/plastics-the-facts-2019/ (accessed on 8 October 2020).

3.   Plastics Europe. Plastics in Packaging. Available online: https://www.plasticseurope.org/en/about-plastics/packaging (accessed on 6 October 2020).

4.   Royal Society. Plastics in the Environment. Available online: https://www.royalsociety.org.nz/major-issues-and-projects/plastics (accessed on 6 October 2020).

5.   Pongrácz, E. The environmental impacts of packaging. In *Environmentally Conscious Materials and Chemicals Processing*; Kutz, M., Ed.; Wiley: Hoboken, NJ, USA, 2007; pp. 237–278. [CrossRef]

6.   Ferreira, A.R.V.; Alves, V.D.; Coelhoso, I.M. Polysaccharide-based membranes in food packaging applications. *Membranes* **2016**, *6*, 22. [CrossRef] [PubMed]

7.   Ritchie, H.; Roser, M. Our World in Data. Available online: https://ourworldindata.org/plastic-pollution (accessed on 8 October 2020).

8.   Donato, P.D.I.; Poli, A.; Taurisano, V.; Nicolaus, B. Polysaccharides: Applications in Biology and Biotechnology/Polysaccharides from Bioagro-Waste New Biomolecules-Life. In *Polysaccharides*; Ramawat, K., Mérillon, J.M., Eds.; Springer: Cham, Switzerland, 2014; pp. 1–29. [CrossRef]

9.   Calva-Estrada, S.J.; Jiménez-Fernández, M.; Lugo-Cervantes, E. Protein-Based Films: Advances in the Development of Biomaterials Applicable to Food Packaging. *Food Eng. Rev.* **2019**, *11*, 78–92. [CrossRef]

10.   Ferreira, A.R.V.; Bandarra, N.M.; Moldão-Martins, M.; Coelhoso, I.M.; Alves, V.D. FucoPol and chitosan bilayer films for walnut kernels and oil preservation. *LWT* **2018**, *91*, 34–39. [CrossRef]

11.   Nešić, A.; Cabrera-Barjas, G.; Dimitrijević-Branković, S.; Davidović, S.; Radovanović, N.; Delattre, C. Prospect of polysaccharide-based materials as advanced food packaging. *Molecules* **2020**, *25*, 135. [CrossRef]

12.   Vieira, T.M.; Moldão-Martins, M.; Alves, V.D. Design of chitosan and alginate emulsion-based formulations for the production of monolayer crosslinked edible films and coatings. *Foods* **2021**, *10*, 1654. [CrossRef]

13.   Ilyas, R.A.; Aisyah, H.A.; Nordin, A.H.; Ngadi, N.; Zuhri, M.Y.M.; Asyraf, M.R.M.; Sapuan, S.M.; Zainudin, E.S.; Sharma, S.; Abral, H.; et al. Natural-Fiber-Reinforced Chitosan, Chitosan Blends and Their Nanocomposites for Various Advanced Applications. *Polymers* **2022**, *14*, 874. [CrossRef]

14.   Ilyas, R.A.; Zuhri, M.Y.M.; Norrrahim, M.N.F.; Misenan, M.S.M.; Jenol, M.A.; Samsudin, S.A.; Nurazzi, N.M.; Asyraf, M.R.M.; Supian, A.B.M.; Bangar, S.P.; et al. Natural Fiber-Reinforced Polycaprolactone Green and Hybrid Biocomposites for Various Advanced Applications. *Polymers* **2022**, *14*, 182. [CrossRef]

15.   Sadeghi, A.; Razavi, S.M.A.; Shaharampour, D. Fabrication and characterization of biodegradable active films with modified morphology based on polycaprolactone-polylactic acid-green tea extract. *Int. J. Biol. Macromol.* **2022**, *205*, 341–356. [CrossRef]

16.   Ilyas, R.A.; Zuhri, M.Y.M.; Aisyah, H.A.; Asyraf, M.R.M.; Hassan, S.A.; Zainudin, E.S.; Sapuan, S.M.; Sharma, S.; Bangar, S.P.; Jumaidin, R.; et al. Natural Fiber-Reinforced Polylactic Acid, Polylactic Acid Blends and Their Composites for Advanced Applications. *Polymers* **2022**, *14*, 202. [CrossRef]

17.   Velickova, E.; Winkelhausen, E.; Kuzmanova, S.; Alvez, V.D.; Moldão-Martins, M. Impact of chitosan-beeswax edible coatings on the quality of fresh strawberries (*Fragaria ananassa* cv *Camarosa*) under commercial storage conditions. *LWT* **2013**, *52*, 80–92. [CrossRef]

18.   Yousuf, B.; Sun, Y.; Wu, S. Lipid and Lipid-containing Composite Edible Coatings and Films. *Food Rev. Int.* **2021**, 1–24. [CrossRef]

19.   Mohamed, S.A.A.; El-Sakhawy, M.; El-Sakhawy, M.A.M. Polysaccharides, Protein and Lipid -Based Natural Edible Films in Food Packaging: A Review. *Carbohydr. Polym.* **2020**, *238*, 116–178. [CrossRef] [PubMed]

20.   Schädel, C.; Richter, A.; Blöchl, A.; Hoch, G. Hemicellulose concentration and composition in plant cell walls under extreme carbon source-sink imbalances. *Physiol. Plant.* **2010**, *139*, 241–255. [CrossRef]

21.   Mendez-Encinas, M.A.; Carvajal-Millan, E.; Rascon-Chu, A.; Astiazaran-Garcia, H.F.; Valencia-Rivera, D.E. Ferulated Arabinoxylans and Their Gels: Functional Properties and Potential Application as Antioxidant and Anticancer Agent. *Oxid. Med. Cell. Longev.* **2018**, *2018*, 2314759. [CrossRef] [PubMed]

22.   Börjesson, M.; Westman, G.; Larsson, A.; Ström, A. Thermoplastic and Flexible Films from Arabinoxylan. *ACS Appl. Polym. Mater.* **2019**, *1*, 1443–1450. [CrossRef]

23.   Serra, M.; Weng, V.; Coelhoso, I.M.; Alves, V.D.; Brazinha, C. Purification of arabinoxylans from corn fiber and preparation of bioactive films for food packaging. *Membranes* **2020**, *10*, 95. [CrossRef] [PubMed]

24.   Péroval, C.; Debeaufort, F.; Despré, D.; Voilley, A. Edible arabinoxylan-based films. 1. Effects of lipid type on water vapor permeability, film structure, and other physical characteristics. *J. Agric. Food Chem.* **2002**, *50*, 3977–3983. [CrossRef]

25.   Ali, U.; Bijalwan, V.; Basu, S.; Kesarwani, A.K.; Mazumder, K. Effect of β-glucan-fatty acid esters on microstructure and physical properties of wheat straw arabinoxylan films. *Carbohydr. Polym.* **2017**, *161*, 90–98. [CrossRef]

26.   Weng, V.; Brazinha, C.; Coelhoso, I.M.; Alves, V.D. Decolorization of a corn fiber arabinoxylan extract and formulation of biodegradable films for food packaging. *Membranes* **2021**, *11*, 321. [CrossRef]

27.   Ferreira, A.R.V.; Torres, C.A.V.; Freitas, F.; Sevrin, C.; Grandfils, C.; Reis, M.A.M.; Alves, V.D.; Coelhoso, I.M. Development and characterization of bilayer films of FucoPol and chitosan. *Carbohydr. Polym.* **2016**, *147*, 8–15. [CrossRef]

28.   Aguirre-Loredo, R.Y.; Rodríguez-Hernández, A.I.; Chavarría-Hernández, N. Physical properties of emulsified films based on chitosan and oleic acid. *CYTA—J. Food* **2014**, *12*, 305–312. [CrossRef]

29.   Chen, G.; Zhang, B.; Zhao, J. Dispersion process and effect of oleic acid on properties of cellulose sulfate-oleic acid composite film. *Materials* **2015**, *8*, 2346–2360. [CrossRef]

30. Moreirinha, C.; Vilela, C.; Silva, N.H.C.S.; Pinto, R.J.B.; Almeida, A.; Rocha, M.A.M.; Coelho, E.; Coimbra, M.A.; Silvestre, A.J.D.; Freire, C.S.R. Antioxidant and antimicrobial films based on brewers spent grain arabinoxylans, nanocellulose and feruloylated compounds for active packaging. *Food Hydrocoll.* **2020**, *108*, 105836. [CrossRef]

31. Bajić, M.; Ročnik, T.; Oberlintner, A.; Scognamiglio, F.; Novak, U.; Likozar, B. Natural plant extracts as active components in chitosan-based films: A comparative study. *Food Packag. Shelf Life* **2019**, *21*, 100365. [CrossRef]

32. Alves, V.D.; Costa, N.; Coelhoso, I.M. Barrier properties of biodegradable composite films based on kappa-carrageenan/pectin blends and mica flakes. *Carbohydr. Polym.* **2010**, *79*, 269–276. [CrossRef]

33. Velickova, E.; Winkelhausen, E.; Kuzmanova, S.; Moldão-Martins, M.; Alves, V.D. Characterization of multilayered and composite edible films from chitosan and beeswax. *Packag. Technol. Sci.* **2013**, *21*, 83–93. [CrossRef]

34. Weller, C.L.; Gennadios, A.; Saraiva, R.A.; Weller, C.L.; Saraiva, R.A. Edible Bilayer Films from Zein and Grain Sorghum Wax or Carnauba Wax. *LWT* **1998**, *21*, 279–285. [CrossRef]

35. Slavutsky, A.M.; Gamboni, J.E.; Bertuzzi, M.A. Formulation and characterization of bilayer films based on Brea gum and Pectin. *Braz. J. Food Technol.* **2018**, 21. [CrossRef]

36. Cazón, P.; Velazquez, G.; Ramírez, J.A.; Vázquez, M. Polysaccharide-based films and coatings for food packaging: A review. *Food Hydrocoll.* **2017**, *68*, 136–148. [CrossRef]

37. Gontard, N.; Thibault, R.; Cuq, B.; Guilbert, S. Influence of Relative Humidity and Film Composition on Oxygen and Carbon Dioxide Permeabilities of Edible Films. *J. Agric. Food Chem.* **1996**, *44*, 1064–1069. [CrossRef]

38. Ghasemlou, M.; Khodaiyan, F.; Oromiehie, A.; Yarmand, M.S. Characterization of edible emulsified films with low affinity to water based on kefiran and oleic acid. *Int. J. Biol. Macromol.* **2011**, *49*, 378–384. [CrossRef] [PubMed]

39. Yu, H.; Gong, L.; Qu, Z.; Hao, P.; Liu, J.; Fu, L. Wettability enhancement of hydrophobic artificial sandstones by using the pulsed microwave plasma jet. *Colloids Interface Sci. Commun.* **2020**, *36*, 100266. [CrossRef]

40. Fabra, M.J.; Talens, P.; Gavara, R.; Chiralt, A. Barrier properties of sodium caseinate films as affected by lipid composition and moisture content. *J. Food Eng.* **2012**, *109*, 372–379. [CrossRef]